Regular Article

blood

RED CELLS, IRON, AND ERYTHROPOIESIS

Novel mechanisms of PIEZO1 dysfunction in hereditary xerocytosis

Edyta Glogowska,[1] Eve R. Schneider,[2] Yelena Maksimova,[1] Vincent P. Schulz,[1] Kimberly Lezon-Geyda,[1] John Wu,[3] Kottayam Radhakrishnan,[4] Siobán B. Keel,[5] Donald Mahoney,[6] Alison M. Freidmann,[7] Rachel A. Altura,[8] Elena O. Gracheva,[2,9,10] Sviatoslav N. Bagriantsev,[2] Theodosia A. Kalfa,[11] and Patrick G. Gallagher[1,12,13]

[1]Department of Pediatrics and [2]Department of Cellular and Molecular Physiology, Yale University School of Medicine, New Haven, CT; [3]Division of Hematology, Oncology and Bone Marrow Transplant, Department of Pediatrics, University of British Columbia, Vancouver, BC, Canada; [4]Department of Paediatric Haematology/Oncology, Children's Cancer Centre, Monash Children's Hospital, Melbourne, VIC, Australia; [5]Division of Hematology, Department of Medicine, University of Washington, Seattle, WA; [6]Section of Hematology/Oncology, Department of Pediatrics, Baylor College of Medicine, Texas Children's Hospital, Houston, TX; [7]Division of Pediatric Hematology and Oncology, Department of Pediatrics, Massachusetts General Hospital, Boston, MA; [8]Division of Pediatric Hematology-Oncology, Department of Pediatrics, Warren Albert School of Medicine, Brown University, Providence, RI; [9]Department of Neuroscience and [10]Program in Cellular Neuroscience, Neurodegeneration and Repair, Yale University, New Haven, CT; [11]Cancer and Blood Diseases Institute, Children's Hospital Medical Center, Cincinnati, OH; and [12]Department of Pathology and [13]Department of Genetics, Yale University School of Medicine, New Haven, CT

Key Points

- There is heterogeneity in the clinical, laboratory, and genetic bases of HX.
- Alterations in PIEZO1 channel kinetics, response to osmotic stress, and membrane trafficking may contribute to channel dysfunction in HX.

Mutations in PIEZO1 are the primary cause of hereditary xerocytosis, a clinically heterogeneous, dominantly inherited disorder of erythrocyte dehydration. We used next-generation sequencing–based techniques to identify *PIEZO1* mutations in individuals from 9 kindreds referred with suspected hereditary xerocytosis (HX) and/or undiagnosed congenital hemolytic anemia. Mutations were primarily found in the highly conserved, COOH-terminal pore-region domain. Several mutations were novel and demonstrated ethnic specificity. We characterized these mutations using genomic-, bioinformatic-, cell biology–, and physiology-based functional assays. For these studies, we created a novel, cell-based in vivo system for study of wild-type and variant PIEZO1 membrane protein expression, trafficking, and electrophysiology in a rigorous manner. Previous reports have indicated HX-associated PIEZO1 variants exhibit a partial gain-of-function phenotype with generation of mechanically activated currents that inactivate more slowly than wild type, indicating that increased cation permeability may lead to dehydration of PIEZO1-mutant HX erythrocytes. In addition to delayed channel inactivation, we found additional alterations in mutant PIEZO1 channel kinetics, differences in response to osmotic stress, and altered membrane protein trafficking, predicting variant alleles that worsen or ameliorate erythrocyte hydration. These results extend the genetic heterogeneity observed in HX and indicate that various pathophysiologic mechanisms contribute to the HX phenotype. (*Blood*. 2017;130(16):1845-1856)

Introduction

The hereditary xerocytosis (HX) syndromes are a group of dominantly inherited disorders of erythrocyte dehydration.[1] HX erythrocytes exhibit decreased total cation and potassium content not accompanied by a proportional net gain of sodium and water. HX patients typically exhibit mild to moderate compensated hemolytic anemia, with variable complications including hydrops fetalis, hemolytic and aplastic episodes, thromboses, gallstones, and propensity for iron overload as an adult.[2,3] Laboratory findings include increased mean corpuscular hemoglobin concentration (MCHC), decreased osmotic fragility, and a characteristic pattern on osmotic gradient ektacytometry,[4] all reflecting cellular dehydration.[5]

Most cases of HX are associated with mutations in PIEZO1, a pore-forming channel that mediates mechanotransduction in mammalian cells, indicating that PIEZO1 plays an important role in maintaining erythrocyte volume homeostasis.[2,6-10] Most, but not all, HX-associated PIEZO1 variants have been shown to exhibit a partial gain-of-function phenotype with generation of mechanically activated (MA) currents that inactivate more slowly than wild type in cell model systems.[2,6,8,11] This indicates that increased cation permeability may lead to dehydration of PIEZO1-mutant HX erythrocytes.

We studied patients from 9 kindreds referred with suspected HX or undiagnosed congenital hemolytic anemia. After identifying mutations in the *PIEZO1* gene, we characterized the mutations in a series of assays, including a novel, cell-based in vivo system we created for study of PIEZO1 membrane protein expression, trafficking, and electrophysiology in a rigorous manner. We identified a number of physiologic and other pathologic abnormalities associated with mutant channels. Variant alleles were identified that are predicted to worsen or ameliorate erythrocyte hydration and influence clinical severity. These results further demonstrate the genetic variability in HX and indicate that mechanisms of channel dysfunction in addition to delayed inactivation contribute to the HX phenotype.

Submitted 19 May 2017; accepted 6 July 2017. Prepublished online as *Blood* First Edition paper, 17 July 2017; DOI 10.1182/blood-2017-05-786004.

The online version of this article contains a data supplement.

The publication costs of this article were defrayed in part by page charge payment. Therefore, and solely to indicate this fact, this article is hereby marked "advertisement" in accordance with 18 USC section 1734.

Methods

Patients

Patients were referred with suspected HX and/or undiagnosed congenital hemolytic anemia.

All studies were approved by an institutional review board. Written informed consent was obtained from the patients or their parents.

Whole-exome sequencing and targeted capture

Whole-exome sequencing (WES), including sequence analyses, was performed as described.[12] Targeted capture was performed as described.[13] All variants were validated by Sanger sequencing. Additional details are provided in supplemental Methods (available on the *Blood* Web site).

A cell-based model system for study of PIEZO1

Wild-type or mutant doxycycline-inducible, PIEZO1-expressing HEK293 cell lines were created using the Flp-In T-Rex system. Stable, single-site integration was verified by Southern blot, messenger RNA (mRNA) expression was validated by quantitative reverse transcription–polymerase chain reaction (RT-PCR), and protein expression was validated by western blot.

Physiologic studies

MA currents were measured in induced and uninduced HEK293 cells expressing wild-type or mutant PIEZO1 and mock-transfected cells. Force was applied to the cell surface by a glass probe mounted on a piezoelectric-driven actuator (Physik Instrumente) in a series of 150-millisecond mechanical steps, in 1-μm increments, while monitoring transmembrane currents at −80 mV in the whole-cell mode as described.[14,15] MA inward currents, apparent threshold of mechanical activation, and time constant of inactivation, obtained by fitting the inactivating component of the mechanocurrent to the monoexponential equation, were monitored. Additional details are provided in supplemental Methods.

Osmotic studies

MA currents measured in the whole-cell mode in induced and uninduced HEK293 cells expressing wild-type or mutant PIEZO1 and mock-transfected cells and membrane stretch were assessed as in the previous section after hypotonic stress, achieved via perfusion of the cells with extracellular media of osmolality from 300 mOsm (isotonic) to 200 mOsm (hypotonic) for 5 minutes then back to 300 mOsm.[16,17]

Immunofluorescence and confocal microscopy

For immunofluorescence (IF), cells grown on glass cover slips were fixed with paraformaldehyde, washed, and a series of permeabilization, blocking, and washing steps performed, including incubation to primary antibody and fluorescently conjugated antibodies.[17] Additional details are provided in supplemental Methods. Samples were examined by confocal microscopy using a Zeiss laser confocal LSM 710 NLO microscope.

Quantitative fluorescent western blotting

Ghosts were prepared from mature erythrocytes of HX patients, denatured, electrophoresed, then transferred to low-fluorescence polyvinylidene fluoride membranes. These were hybridized to anti-PIEZO1, anti-α-spectrin (control), and anti-actin (control) antibodies. Gels were imaged and data quantified. Additional details are provided in supplemental Methods.

Results

Patients

We studied patients from 9 kindreds with suspected HX (Table 1). The predominant clinical and laboratory findings were splenomegaly and hemolytic anemia with reticulocytosis (Table 1). In utero manifestations were observed in 3 kindreds. One HX mother who suffered from nonimmune hydrops fetalis (NIHF) as a fetus subsequently carried an affected fetus who also suffered from NIHF. Several patients required blood transfusion at some time during their life. Iron overload, found in 3 patients, was severe enough to require chelation in 2. Of the 3, only 1 patient (number 4; Table 1) had a significant history of transfusion. One patient (number 9) died suddenly at age 25 years; autopsy revealed cardiac iron overload.

Targeted capture, exome sequencing, and variant identification

WES or targeted capture identified 6 missense or indel mutations of the *PIEZO1* gene in probands from all 9 kindreds (Table 2). At least 3 mutation prediction algorithms predicted that the 4 missense mutations were deleterious for protein function, and all 4 had highly significant combined annotation-dependent depletion (CADD) Phred scores ≥15, with 2 over 30 (Table 2), predicting pathogenic variants.[18] Three of the 6 variants are novel and are not present in the 1000 Genomes, Exome Variant Server, or Exome Aggregation Consortium (ExAC) databases. The fourth variant, p.Leu2495_Glu2496dup (also known as E2496ELE), which we found in 4 kindreds, although not in the 1000 Genomes, Exome Variant Server, or ExAC databases, has been found in over a dozen unrelated HX kindreds.[8,19] Patient 3, who previously was described to have a deleterious mutation in the Gardos channel, *KCNN4*, was found to have a homozygous, in-frame deletion in *PIEZO1* (Table 2). No other mutations were detected in *KCNN4* or *SLC4A1* in any of the patients. The presence of each mutation was confirmed by Sanger sequencing (not shown).

Based on computer modeling, 4 of these mutations were located primarily in the COOH terminus, the region that dictates pore properties of PIEZO1 (Figure 1A).[20] Recently, cryoelectron microscopy of a region of mouse Piezo1 at a resolution of 4.8 Å demonstrated that Piezo1 forms a trimeric propeller-like structure, with the extracellular domains resembling 3 peripheral blades and a central cap, with a central region that encloses a potential ion-conducting pore.[21] It was suggested that force-induced motion of the peripheral blades or peripheral helices led to conformational changes and channel gating. Only 4 of our mutants were included in the reported structure: R2088G, R2302H, R2488Q, and E2496ELE. Notably, R2488Q is at the top of the cap of the predicted pore, and E2496ELE is at the junction of the α2 and α3 intracellular COOH-terminal domains, a region predicted to participate in formation of the pore module.[21,22] As expected for residues in this functional COOH-terminal region of PIEZO1,[23] these 4 amino acids are highly conserved across species (Figure 1B).

A cell-based model system for study of PIEZO1

To study mechanisms of mutant PIEZO1 dysfunction, we created an in vivo system for study of wild-type and mutant PIEZO1 in functional, cell-based assays. We used the Flp-In T-Rex system to generate stable mammalian HEK293 cell lines with doxycycline-inducible expression of human PIEZO1. This system allows expression of PIEZO1 in stably-transfected, single-copy HEK293 cells with a uniform integration site, allowing rigorous comparison of variant proteins with wild type. Adding rationale to development of this model, a previous study of the function of the PIEZO1 M2225R variant in transiently transfected HEK293 cells was confounded by changes due to variations introduced by transient transfections.[8] We have used this system to demonstrate critical differences in cell lines expressing KCl cotransporters with alterations in a single amino acid.[17] For wild type and each mutant, we developed 2 functional HEK293 cell PIEZO1 models, with or without a COOH-terminal 3X FLAG tag. HEK293 cells have been shown to be an excellent model for study of PIEZO1 function.[14,15] PIEZO1 has

Table 1. Clinical and laboratory features of HX patients

Patient	Sex	Inheritance	NIHF	Perinatal anemia	Any transfusion	Enlarged spleen	Splenectomy/ cholecystectomy	Hb, g/dL	MCV, fL	MCH, pg	MCHC, g/dL	Retic count, %	T bili, mg/dL	OF	Ekta-cytometry	RBC electrolytes	Ferritin/ chelation	Mutation
1	F	Unknown	No	No	No	Yes	No/yes	10	29	35.6	34.8	2.8	1.9	NI	No	ND	1087/yes	R1943Q
2	F	Unknown	No	No	No	No	No/no	13.9	86	NR	38.3	10	5.2	NI	Yes	Na 56, K 208	NR	R2088G
3	M	De novo	Yes	No	Yes	Yes	No/yes	9.9	108	36	ND	6.4	2.2	ND	No	Na 16, K 81	295	R2488Q
4	F	AD*	No	No	Yes	Yes	No/no	9.3	79.7	28.5	35.7	3.2	3.8	NI	Yes	ND	1240/yes	R2302H
5	F	AD	NR	NR	Yes	Yes	Yes/yes	10	106	37.6	36.4	25	NR	Dec	No	Na 18.6, K 59.1	NR	K1877del
6	F	Unknown	Yes	Yes	Yes	Yes	No/no	12.5	95.4	35.8	37.5	11.8	1.3	Both	No	ND	NR	E2496ELE
7	M	AD	No	No	No	Yes	No/no	10.6	98.3	31.8	32.3	9.6	NR	No	No	ND	126	E2496ELE
8	F	AD	Yes	Yes	Yes	Yes	Yes/yes	10	115	39.5	34.8	4.7	2.5	Dec	Yes	Na 48, K 82	188	E2496ELE
9	F	Unknown	No	No	Yes	Yes	Yes/yes	9.1	125	44	35	8	2.4	No		Na 9.3, K95.1	500	E2496ELE

AD, autosomal dominant; Dec, decreased; F, female; Hb, hemoglobin; M, male; MCH, mean corpuscular hemoglobin; MCHC, mean corpuscular hemoglobin concentration; MCV, mean corpuscular volume; ND, not done; NI, normal; NIHF, nonimmune hydrops fetalis; NR, not reported; OF, osmotic fragility; RBC, red blood cell; Retic, reticulocyte; T bili, total bilirubin.
*Patient with coinherited β-globin variant. See "Results" for details.

been shown to be fully functional when a COOH-terminal tag is added,[14,15] which we have validated (see next section and supplemental Data). The tag allows us to perform trafficking and IF microscopy–based assays. As positive controls, we used lines expressing the original HX-associated PIEZO1 mutations, M2225R and R2456H, which have been shown to demonstrate a delayed inactivation phenotype.[8,11]

We first examined our cell model systems using wild-type PIEZO1 with or without a COOH-terminal 3X FLAG tag. We demonstrated single-copy, single-genomic integration site by Southern blot (not shown), PIEZO1 mRNA expression by quantitative RT-PCR, and protein expression by western blot (supplemental Figure 1), as well as physiologic studies (see next section). Time-course experiments demonstrated significant PIEZO1 protein expression at 16 hours postinduction that persisted up to 96 hours postinduction (Figure 2A). The time frame between 24 and 48 hours postinduction was used for all experiments unless otherwise indicated. IF studies localized PIEZO1 expression to the cell membrane (Figure 2B). We then generated PIEZO1-mutant cell lines with or without FLAG tags and validated expression using comparative analyses (supplemental Figures 1 and 2). No lower-molecular-weight degradation products were detected in wild-type or mutant samples. The HX-associated mutations did not result in a significant decrease in the level of PIEZO1 expressed in HEK293 cells, suggesting the mutations did not cause a significant decrease in protein synthesis or stability.

Physiologic analyses

We measured MA currents in the whole-cell mode in induced and uninduced HEK293 cells expressing wild-type or mutant PIEZO1. MA currents were recorded after applying mechanical force on the cell surface using a glass probe, increasing in 1-μm increments of indentation, while monitoring transmembrane currents at constant voltage. After induction, cells expressing wild-type PIEZO1 with or without a FLAG tag demonstrated a rapid transient increase in current after stimulation, related to the depth of the indenting probe, as previously described (supplemental Figure 3).[8] Uninduced control cells produced no MA current.

Whole-cell currents were then recorded in uninduced and induced mutant PIEZO1-expressing HEK293 cell lines. All induced wild-type and mutant MA inactivation currents could be fitted with a mono-exponential function. Two mutants, R1943Q and E2496ELE, demonstrated an increase in the inactivation time constant, as did 2 previously characterized HX mutants, M2225R and R2456H, included as controls, compared with wild type (Figure 3; Table 3).[2,6,8,11] This is the typical pattern that has been described with HX-associated PIEZO1 missense mutations.[8] These mutants are defined as gain of function, as they prolong channel activity in response to a given mechanical stimulus. The other mutants did not demonstrate a statistically significant increase in inactivation time constant (τ, milliseconds) except for the K1877del mutant which displayed lower τ, indicating faster closing of channel (see next paragraph).

Sensitivity of a channel to mechanical stimulation can be estimated by the minimal indentation measuring the apparent activation threshold for each cell. This can be calculated by establishing the minimal indentation, after cell contact is made, required to activate the channel. We observed differences in threshold for 3 mutants, R2088G, R2302H, and R2488Q (Figure 3C).

Other abnormalities in channel properties were observed. The K1877del mutant exhibited both faster channel-inactivation kinetics compared with wild type (control, $\tau = 6.1 \pm 0.2$ milliseconds vs K1877del, $\tau = 5.3 \pm 0.2$ milliseconds; mean $\pm$ standard error of the mean, $P < .009$, Student t test) and a decrease in current amplitude, with averaged peak current at 6 μm, a value approximately half of wild type

Table 2. Genetic analyses

Mutation	Type	Location	1000G	ExAc	SIFT	LRT	Mutation taster	CADD Phred
NM_001142864:c.G5828A:p.R1943Q	Missense	Exon 41	0.00739	0.0025	0.57	0.096	1	15.18
NM_001142864:c.C6262G:p.R2088G	Missense	Exon 43	0	0	0.18	0	1	32
NM_001142864:c.G7463A:p.R2488Q	Missense	Exon 51	0	4.81E-05	0.02	0	1	35
NM_001142864:c.G6905A:p.R2302H	Missense	Exon 47	0	0.0003	0.37	0	1	28
NM_001142864:c.5632_5634del:p.1878_1878del	Deletion	Exon 39	0.21	0.35	NA	NA	NA	NA
NM_001142864:c.7479_7484dup:p.L2495_E2496dup	Insertion	Exon 51	0	0	NA	NA	NA	NA

SIFT, LRT, Mutation Taster, and CADD scores are from predicted mutation effect scores obtained from the Annovar database (http://annovar.openbioinformatics.org/en/latest/). Scores of 0 are predicted to be damaging by the SIFT and LRT algorithms whereas scores of 1 are predicted to be tolerated. The scale is inverted for the Mutation Taster algorithm.

1000G, Allele frequency in the Thousand Genomes database (http://www.internationalgenome.org/); CADD, combined annotation-dependent depletion; ExAc, ExAc Browser database (http://exac.broadinstitute.org/); LRT, likelihood ratio test; NA, not applicable; SIFT, sorting intolerant from tolerant.

($P < .05$; Figure 4A). The E2496ELE insertion mutant displayed increased inactivation rate compared with wild-type (9.9 ± 0.05, $P < .001$, Student t test). In addition, whereas the wild-type channel inactivated completely, in 77% of records from the mutant, a persistent mechanocurrent was observed, indicating incomplete channel closure (Figure 4B). Interestingly, in comparison, the K1877del mutant brings less excitation per amount of stimulus compared with WT, whereas the E2496ELE mutant brings more.

Osmotic studies

Changes in osmotic pressure, which induce a host of processes in the cell, are frequently used as a stimulus to direct mechanosensation. We tested the sensitivity of wild-type PIEZO1 expressed in HEK293 cells to different environmental osmolality. Initially, we measured changes in cell diameter in wild-type PIEZO1-expressing HEK293 cells with solutions of different tonicity: 300 mOsm, 275 mOsm, 250 mOsm, 200 mOsm, and 150 mOsm. Increases in cell diameter were observed, paralleling the degree of hypotonicity (Figure 5A). To test the mechanosensitivity of PIEZO1 to changes in environmental tonicity, a hypotonic state of 200 mOsm was chosen because it led to cell swelling without cell rupture seen at lower tonicities. We next measured MA currents, applied at 6 μm, in the whole-cell mode in uninduced and induced HEK293 cells in isotonic and hypotonic (200 mOsm) conditions. Three steps of recordings

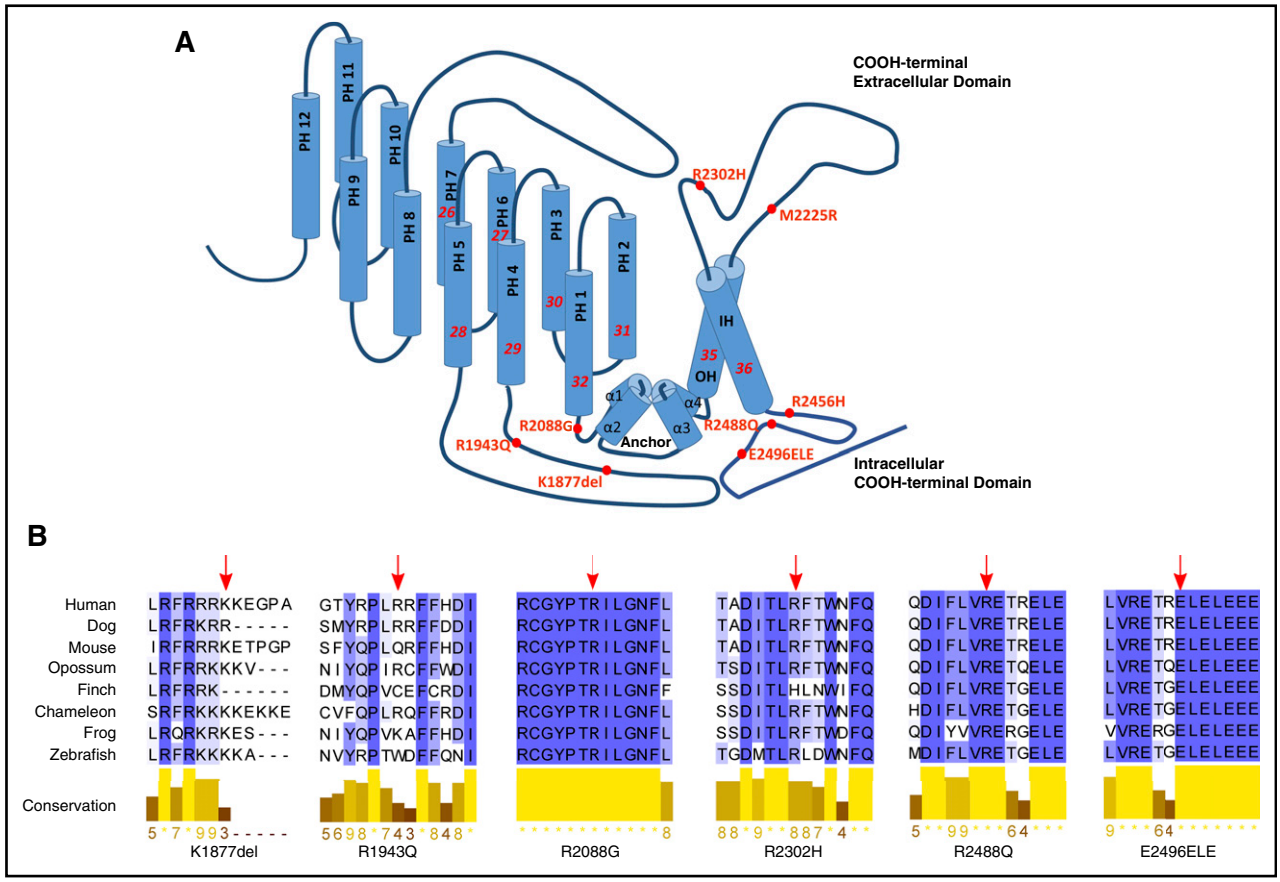

Figure 1. HX-associated PIEZO1 mutations. (A) The position of the 6 PIEZO1 mutations identified in this report and the first 2 HX-associated PIEZO1 mutations described, R2456H and M2225R, are shown on a model of PIEZO1 derived from the cryoelectron microscopy structure.[21] The locations of the channel anchor, the peripheral helices (PH), the inner helices (IH), and the outer helices (OH) are shown. (B) Conservation of HX-associated mutant amino acids. The 4 amino acids located in the COOH-terminal domain containing the putative PIEZO1 channel exhibit high degrees of conservation.

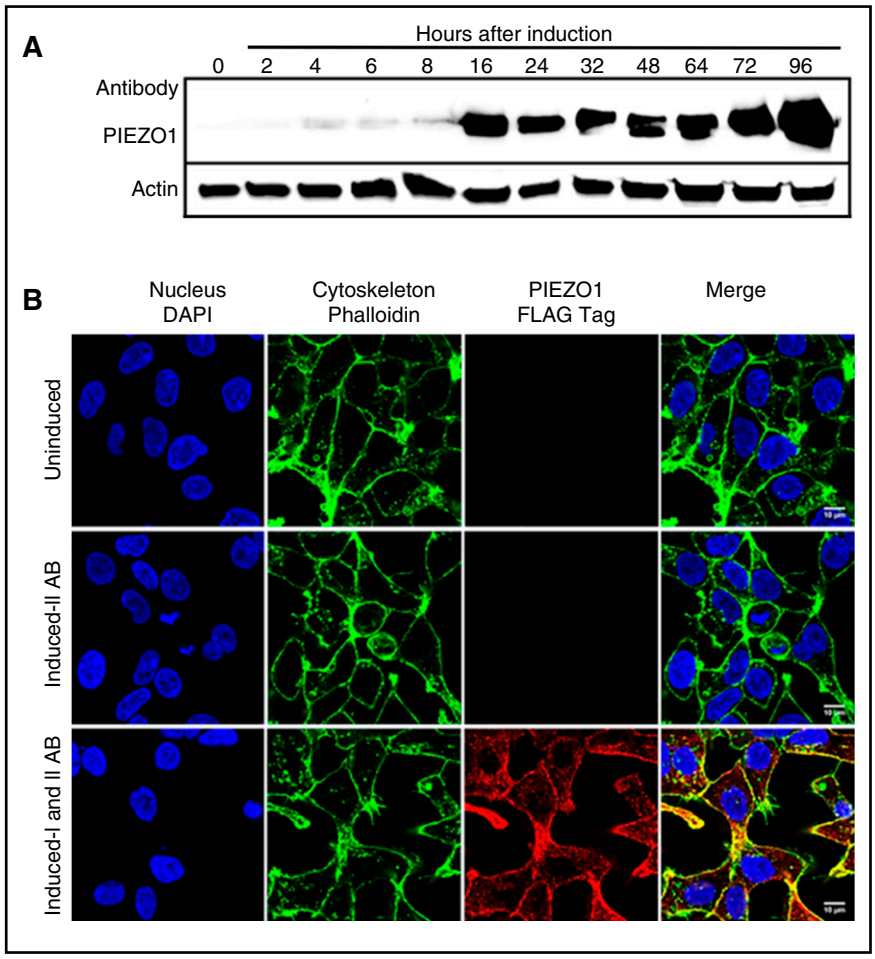

Figure 2. Time course and IF analysis of wild-type PIEZO1 expression in HEK293 cells. (A) Time-course experiments in an HEK293 cells doxycycline-inducible model of PIEZO1 demonstrated significant protein expression beginning at 16 hours and lasting for 96 hours postinduction. The time frame between 24 and 48 hours postinduction was used for all experiments unless otherwise indicated. (B) IF studies localized PIEZO1 expression to the cell membrane after doxycycline induction. 4′,6-Diamidino-2-phenylindole (DAPI) stain of nuclei (blue), phalloidin AF488 stain of F-actin (green), and ATT0647N FLAG-tagged PIEZO1 (red) images in uninduced and induced cells are shown. Scale bars, 10 μM. IAB, primary antibody, mouse anti-FLAG tag ATTO647N; IIAB, secondary antibody, goat anti-mouse; In, induced; Un, uninduced.

(isotonic-hypotonic-isotonic washout) were applied to each cell. There was a dramatic increase in the average peak current of MA currents in hypotonic conditions ($P < .005$; Figure 5B). This hypotonicity-induced increase in amplitude, like that observed in isotonic conditions, was blocked by 30 μM gadolinium chloride (Gd^{3+}) (Figure 5C).

We next tested the sensitivity of HX-associated PIEZO1 mutants expressed in HEK293 cells to different environmental osmolality. Like wild type, the previously described M2225R mutant HX variant, had a marked increase in current amplitude after hypotonic stress. From the mutants in this report, only R2088G demonstrated a similar marked hypotonic-induced increase in current amplitude. Of the remaining mutants, the response to hypotonic stress was blunted in R2488Q and K1877del mutants whereas R2302H and E2496ELE had no response to hypotonic stress (Figure 5D).

Protein expression and membrane trafficking

Mutations in transmembrane proteins that perturb membrane trafficking and membrane protein quality have been associated with a wide variety of genetic diseases, frequently associated with mutation of lysine- or arginine-based endoplasmic reticulum (ER) retention/retrieval signals.[24-28] The HX-associated arginine mutants identified are excellent candidates for an altered trafficking/quality control phenotype, as arginine-based signals may be found in a variety of locations throughout a protein, including the cytosolic NH2 terminus, intracellular loops, and the cytosolic COOH terminus of a protein.[27] We examined mutants for alterations in membrane stability and trafficking in our HEK293 cell model using IF confocal microscopy.

Cells were transfected with ER-GFP, a plasmid that expresses green fluorescent protein (GFP) fused to the ER signal sequence of calreticulin and KDEL (ER retention signal), which stains the ER with minimal cellular disruption. Cells were also stained with antibody against Golgi apparatus, anti-GM130, conjugated with Alexa Fluor 488. We observed that 3 arginine mutants, R2488Q, R2302H, and R2088G, demonstrated partial intracellular retention, colocalizing with ER and Golgi markers despite immunoblotting of whole-cell extracts showing that all 3 mutant proteins were expressed at the same level as wild type (Figure 6). This indicates that despite appropriate amounts of protein synthesis of these mutants as demonstrated in total cellular extracts, the accumulation of mutant PIEZO1 protein in the ER and/or Golgi suggests a defect in vesicular to membrane transport. Interestingly, the 3 mutants that demonstrated altered membrane trafficking also demonstrated no alteration in channel inactivation.

Semiquantitative western blotting was performed using ghosts prepared from the erythrocyte membranes of affected patients. No differences in PIEZO1 expression were observed between ghosts of wild-type or mutant patients normalized against actin expression, α-spectrin expression, or both (supplemental Figure 4A-B). Artifacts introduced by western blotting including transfer efficiency of the very-high molecular PIEZO1 protein and nonlinear signal detection may preclude detection of membrane deficiency as such differences may be beyond the sensitivity of this assay. Perhaps application of sensitive proteomics, such as second-generation multiple reaction

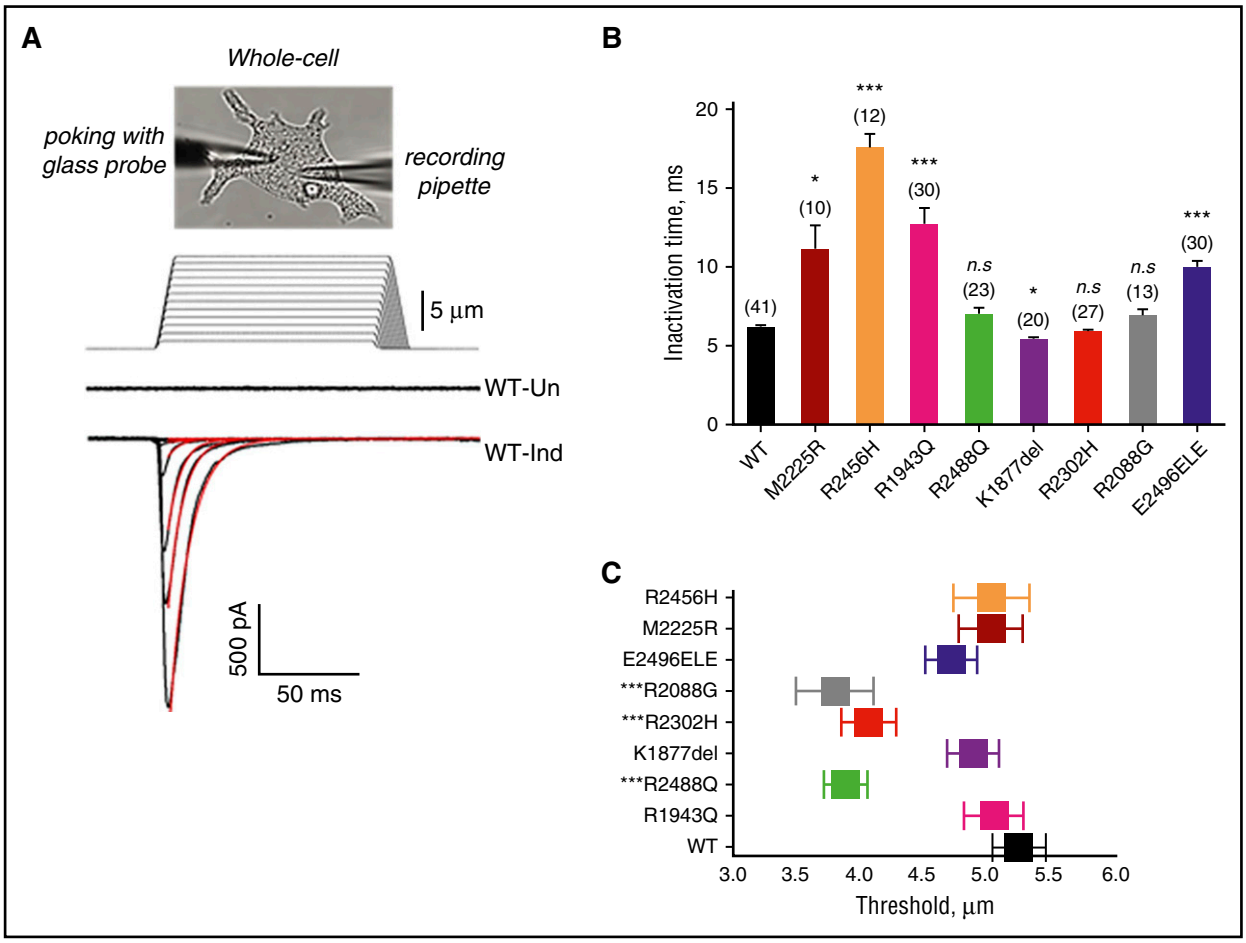

Figure 3. MA currents in HEK293 cells expressing wild-type or mutant PIEZO1. (A) Representative traces of MA inward currents from uninduced (Un) or induced (Ind) stably transfected HEK293 cells expressing wild-type (WT) PIEZO1. Using a patch-clamp electrophysiological technique, functionality of recombinant PIEZO1 channel activity was examined in the whole-cell configuration. Upon a series of mechanical stimulations of a glass probe (1-μm increments, 150-ms step duration), currents were recorded in the whole-cell patch-clamp configuration at holding potential −80 mV. The stimulus waveforms are shown above the current traces. The red lines are MA currents fitted with monoexponential function. (B) Average of inactivation time constant (τ, milliseconds) for wild-type, HX-associated mutant, and known HX-associated mutant (R2456H and M2225R) controls. $^{*}P < .05$ $^{***}P < .001$ (Student *t* test). (C) Threshold of activation. Several of the mutants studied displayed greater sensitivity to mechanical stimulus as indicated by minimal indentation activation threshold. $^{***}P < .001$ (Student *t* test). n.s., not significant.

monitoring–based approaches, will provide insight into PIEZO1 quantitation in mature erythrocytes. Recently, altered PIEZO1 density on epithelial membranes has been shown to alter cellular phenotype.[29] It will be interesting to determine whether erythrocyte membrane density of PIEZO1 proteins influences its function in mature erythrocytes, especially in mutant cells that may exhibit PIEZO1 deficiency.

Morphologic analyses and the E2496ELE mutant

The morphology of wild-type and HX-associated mutant PIEZO1-expressing HEK293 cell lines was examined 48 hours after doxycycline induction. Except for the E2496ELE mutant, there were no major morphologic differences between paired uninduced and

Table 3. Study of hereditary xerocytosis-associated PIEZO1 variants

	Inactivation kinetics			Osmotic phenotype			
Mutation	N	Threshold, μm	Inactivation time constant, T (ms)	n	Fold of amplitude increase relative to osmotic	Comments	Trafficking defect
WT	41	5.3 ± 0.2	6.1 ± 0.2	8	19.1 ± 0.2***	Increase in peak current	None
M2225R	10	5.0 ± 0.2	11.0 ± 0.9*	4	14.2 ± 0.2***	Like WT	None
R2456H	12	5.0 ± 0.3	17.4 ± 1.0***	0	No data	No data	None
R1943Q	30	5.1 ± 0.2	12.6 ± 1.1***	0	No data	No data	None
R2088G	13	3.8 ± 0.3***	6.8 ± 0.5	4	12.1 ± 0.5***	Like WT	Colocalization with ER and Golgi
R2488Q	23	3.9 ± 0.2***	6.9 ± 0.5	8	4.2 ± 0.1*	Blunted response	Colocalization with ER and Golgi
R2302H	27	4.1 ± 0.2***	5.8 ± 0.2	6	0.3 ± 0.1	No response	Colocalization with ER and Golgi
K1877del	20	4.9 ± 0.2	5.3 ± 0.2*	6	3.2 ± 0.1*	Blunted response	None
E2496ELE	30	4.7 ± 0.2	9.9 ± 0.5***	4	0.9 ± 0.1	No response	None

Values are mean ± standard error of the mean unless otherwise indicated.
ER, endoplasmic reticulum; n, number of experiments; N, number of tested cells; WT, wild type.
$^{*}P < 0.05$; $^{***}P < 0.001$ (Student *t* test).

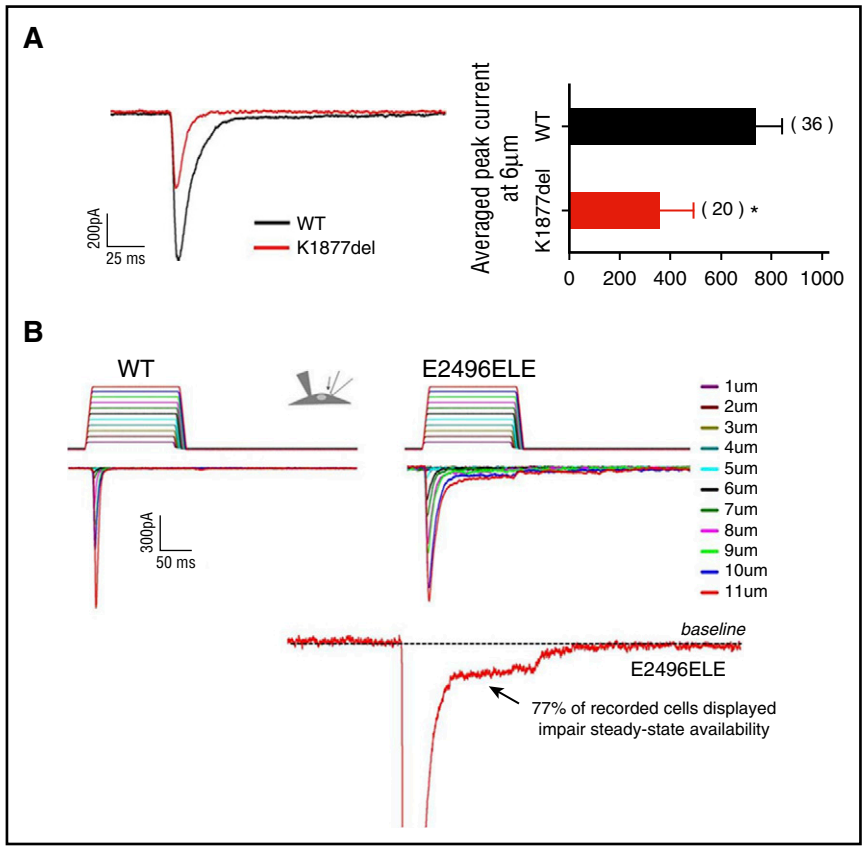

Figure 4. Altered channel kinetics exhibited by PIEZO1 mutants. MA currents in HEK293 cells expressing wild-type or mutant PIEZO1 were examined using a whole-cell patch-clamp technique. (A) K1877del mutant. Left panel, representative traces of peak current amplitude of MA wild-type and PIEZO1-K1877del cells. Both faster channel kinetics and smaller peak current amplitude were observed for the K1877del mutant. Right panel, a comparison of averaged peak currents amplitude recorded at 6 μm from wild-type and K1877del mutant cells, with the K1877del mutant showing a significant decrease of peak current. (B) E2496ELE mutant. Representative traces of MA currents in wild-type (left) and PIEZO1-E2496ELE mutant (right) cells, as a function of depth of the indenting probe. The stimulus waveforms used in activation protocol are shown above the traces with the colors corresponding to each depth of indentation. The E2496ELE insertion mutant displayed increased inactivation rate compared with wild type. In addition, whereas wild-type channel inactivated completely, in 77% of records from the mutant, persistent mechanocurrent was observed, indicating incomplete channel closure. Bottom panel, a current recorded from an E2496ELE mutant at 11 μm displaying increased steady-state availability of the channel shown by the interruption in inactivating current. For presentation, a zoomed in view of the interrupted region is shown with the current peak cutoff.

induced cells. After induction, the E2496ELE mutant demonstrated cell swelling, rolling up of cell edges, and detachment from the plate.

Because there was a morphologic phenotype with the E2496ELE mutant, and because it is one of the most commonly identified HX-associated PIEZO1 mutations, we performed additional studies. In a time-course experiment with constant recording, these cells demonstrated morphological changes as early as 16 hours postinduction with swelling and rounding up of cell edges, followed by wide-scale detachment of cells from the plate by 48 hours (Figure 7A; supplemental Video 1; supplemental Figure 5). Beginning at 48 hours postinduction, live cell numbers determined by CCK8 staining dramatically decreased and mutant cells began to undergo apoptosis as determined by annexin V binding (Figure 7B).

Attempts to block this process by the addition of various inhibitors, including 4 μM *Grammostola spatulata* mechanotoxin (GsMTx4), 30 μM gadolinium, or 30 μM ruthenium red, yielded limited to no change in cell swelling, detachment, and apoptosis (Figure 7A-B; not shown). It is possible that this mutation leads to conformational changes in the channel and/or interrupt PIEZO1 interactions with cytoskeleton protein(s) responsible for adherence. In addition, these morphologic changes were not altered by performing similar time-course experiments in calcium-free media.

Cotransfection of wild-type, full-length PIEZO1, with enhanced GFP as a marker of transfection, into mutant cells 12 hours prior to induction did not fully rescue the apoptotic, decreased cell number phenotype (supplemental Figure 6). The number of detached cells in suspension was statistically decreased (number of total cells, $P = .01$; number of live cells, $P = .1$). However, the total number of all cells (attached and in suspension) was not statistically different ($P = .1$).

Discussion

Identification of mutations in PIEZO1 as the primary cause of HX has led to both an increased awareness of the disease and an increase in its diagnosis, particularly by genetic-based methodologies. Like the subjects reported here, many HX patients had been labeled with the diagnosis of "congenital anemia" until genetic diagnosis was obtained. This report demonstrates several interesting features of PIEZO1 variants and hematologic disease.

PIEZO1 variants coinherited with other congenital hemolytic anemias may alter the clinical phenotype

In the proband studied from kindred 4, the R2302H PIEZO1 mutant was coinherited with a heterozygous β-thalassemia mutant, β-globin-Cincinnati,[13] predicted to produce an elongated β-chain nearly identical to β-globin Geneva. Although patients with β-globin Geneva exhibited only a chronic, mild microcytic anemia,[30] our patient exhibited transfusion-dependent anemia. Her clinical severity may have been exacerbated by the PIEZO1 R2302H variant which exhibited a trafficking phenotype. A recent report described a young man with HX due to a *PIEZO1* mutation whose erythrocyte dehydration and clinical severity were accentuated by coinheritance of hemoglobin C trait.[31] It is not surprising that deleterious PIEZO1 mutants coinherited with other congenital anemias would worsen the clinical phenotype. Coinherited mutations would especially be predicted to lead to a more severe phenotype in inherited disorders with secondary erythrocyte dehydration, including sickle cell disease, β-thalassemia, hemoglobin C, and hereditary spherocytosis.[1]

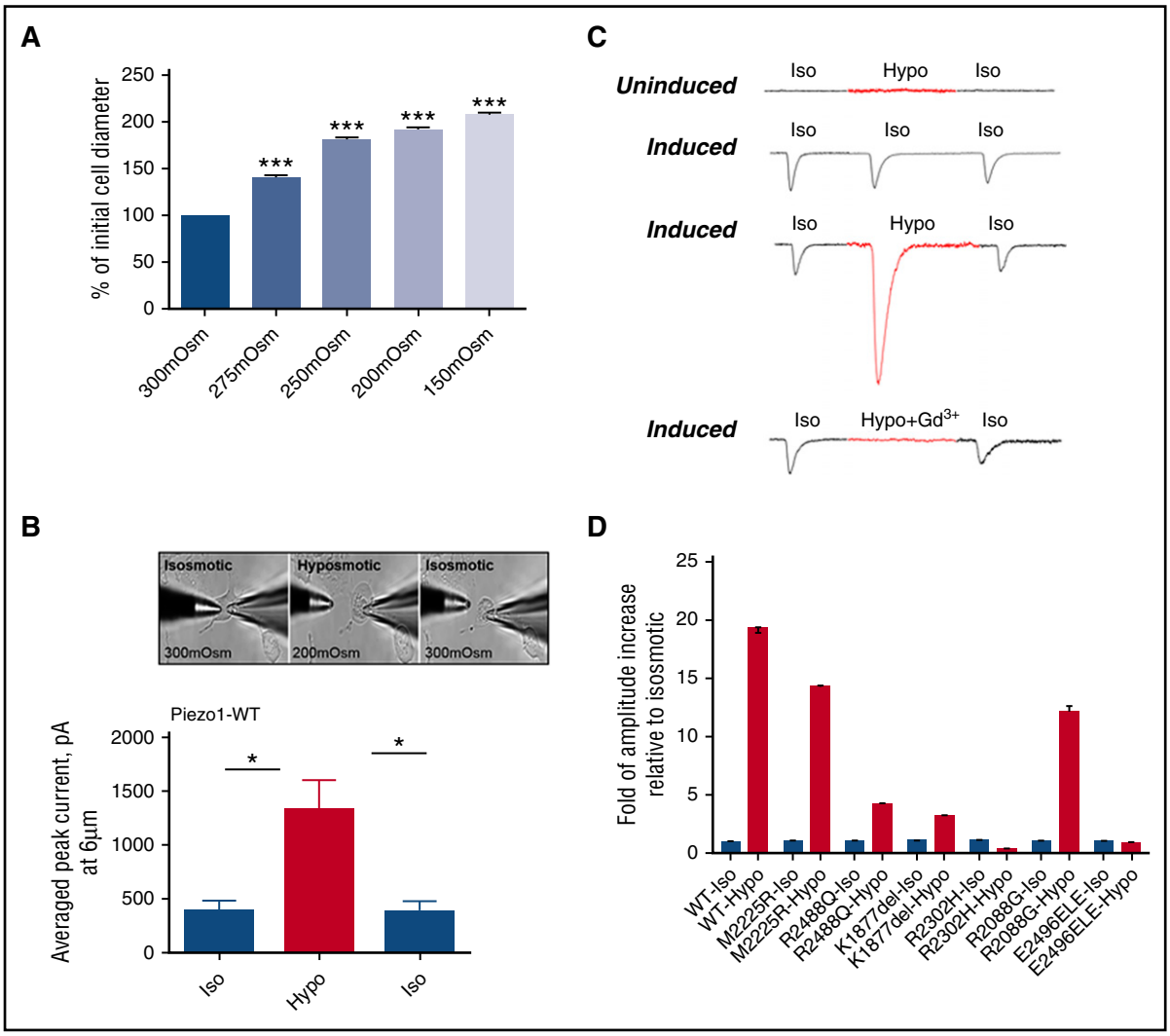

Figure 5. Osmotic stress and PIEZO1 activity. The sensitivity of PIEZO1 expressed in HEK293 cells to different environmental osmolality was analyzed. (A) Changes in cell diameter were measured after solutions of different tonicity were applied to the cell surface; n = 61/Osm, ***$P < .001$. (B-C) MA currents applied at 6 μm were recorded in the whole-cell patch-clamp configuration, at holding potential −80 mV in HEK293 cells expressing wild-type PIEZO1 (uninduced and induced). Recordings were obtained from isotonic (Iso; 300 mOsm) physiological solution, after perfusion with hypotonic (Hypo; 200 mOsm) solution, and after washout with isotonic (Iso; 300 mOsm) solution. The same experiments were performed only with isotonic (300 mOsm) physiological solution as a control. There was a dramatic increase in the average peak current of MA currents in hypotonic conditions ($P < .005$, n = 6). To determine the involvement of PIEZO1 on recorded current responses, 30 μM of the inhibitor gadolinium were added to hypotonic solution. The same experiments were performed only with isosmotic (300 mOsm) physiological solution, as a control. A typical response after the addition of gadolinium is shown. (D) MA currents were similarly measured in HEK293 cells expressing HX-associated mutant PIEZO1 (uninduced and induced), with recordings obtained at isotonic (300 mOsm) and hypotonic (200 mOsm) physiological solutions (Table 3).

Similarly, PIEZO1 variants coinherited with other congenital hemolytic anemias may ameliorate the clinical phenotype. Patient 3, who previously was described to have a deleterious mutation in the Gardos channel, *KCNN4*, was found to have a homozygous, in-frame deletion in *PIEZO1*: K1877del. This variant exhibited decreased current and increased channel kinetics, features predicted to ameliorate the dehydration phenotype. This PIEZO1 variant was identified in an Italian HX kindred with a different mutation of *KCNN4*: R352H.[32] In that kindred, an HX patient who coinherited the K1877del PIEZO1 allele exhibited less erythrocyte dehydration than another family member who did not.

Some PIEZO1 variants are common, especially in specific ethnic groups

In northern European populations, 2 HX-associated *PIEZO1* variants, the originally described R2456H mutant, and the E2496ELE found in 4 unrelated kindreds in our study, appear to be among the most common variants found in typical HX patients.[6-10] Haplotype analyses reveal that the E2496ELE mutation is found on at least 4 different haplotypes.[6]

One PIEZO1 mutant in our study, R1943Q, was identified in an African American woman with a typical HX phenotype. This variant, classified as rs115799619, is a relatively common allele in Africans with an allele frequency of 0.02 in both 1000 Genomes and ExAc. It is African specific and there are no rs115799619 homozygotes in 1000 Genomes or ExAc, despite its frequency. The K1877 deletion is common in Europeans with an allele frequency of 0.39, whereas the allele frequency is 0.14 in Africans and 0.08 in East Asians. Like other reports, 3 of the variants in this report are novel and 1 occurred de novo. Given the large size of the *PIEZO1* gene, it is not surprising that new HX-associated mutations continue to be identified, including those that occur de novo, contributing to the genetic heterogeneity seen in the HX syndromes.

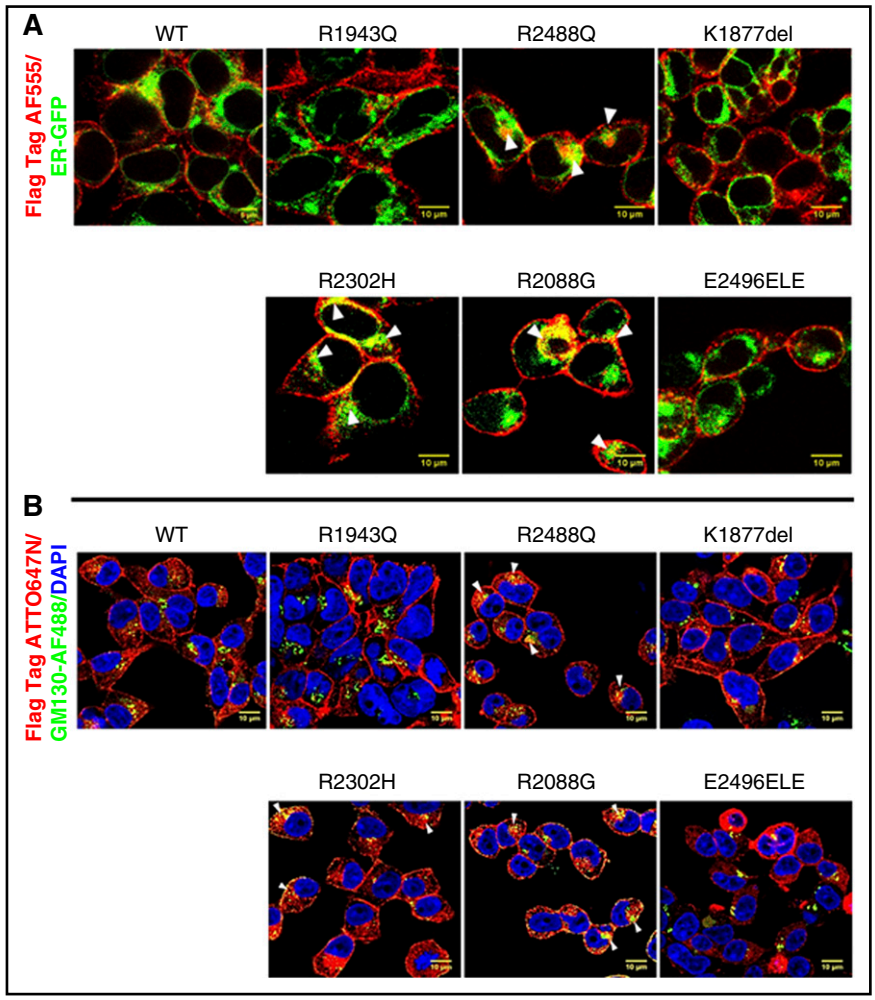

Figure 6. Cellular localization of wild-type and mutant PIEZO1 determined by IF confocal microscopy. (A) Wild-type and mutant FLAG-tagged PIEZO1-expressing HEK293 cells were transfected with ER-GFP, a plasmid that expresses GFP fused to the ER signal sequence of calreticulin and KDEL (ER retention signal). Cells were stained with anti-FLAG AF555 (red) and anti-GFP (green). (B) Wild-type and mutant FLAG-tagged PIEZO1-expressing HEK293 cells were stained with anti-FLAG ATT0647N (red), DAPI (blue), and an antibody against Golgi apparatus, anti-GM130, conjugated with Alexa Fluor 488 (green). Three arginine mutants, R2488Q, R2302H, and R2088G, demonstrated partial intracellular retention, colocalizing with ER and Golgi markers. Scale bars, 10 μm.

Some PIEZO1 variants exhibit defective membrane trafficking

Defects in membrane trafficking of ion channels linked to hereditary hemolytic anemia have been described in band 3, the anion exchanger (*SLC4A1*), in patients with dominant hereditary spherocytosis.[26] A series of band 3 variant alleles, many with juxtamembrane arginine mutations similar to the PIEZO1 mutants, exhibited defective folding and retention in the ER–Golgi-intermediate compartment–*cis* Golgi transport pathway. Frequently, misfolded mutants have abnormally long contact with ER chaperones and then are degraded. To better understand PIEZO1 trafficking, it will be important to identify PIEZO1 chaperones, as well as to determine whether PIEZO1 dimerizes or trimerizes in the ER during its synthesis and if this oligomerization is critical for its folding and membrane trafficking.[26,33,34] In some dominant disorders, not only are mutant homozygous heteromeric proteins mistrafficked, but also wild-type-mutant heteromeric proteins are retained in the ER, further accentuating the clinical phenotype.

PIEZO1 and erythrocyte volume

Some of the HX-associated PIEZO1 variants tested exhibited an altered phenotype during hypotonic stress. It has been suggested that PIEZO1 plays a role in erythrocyte volume regulation, with PIEZO1-mutant HX erythrocytes gradually becoming dehydrated during their repeated cycles of travel through the microcirculation, associated with changes in oxygenation/deoxygenation.[35] Genetic and physiologic studies implicate a role for PIEZO1 in volume homeostasis. Volume sensing, a poorly understood process in vertebrate cells, has been linked to stretch-activated currents induced by changes in cell volume.[36] As soon as the PIEZO proteins were identified, they were candidates for cellular osmosensors.[37] Physiologic studies have shown that the PIEZO1 blocker, GsMTx4, inhibits both MA currents and whole-cell regulatory volume decreases in NRK-49 cells,[36,38] indicating a role for PIEZO1 in volume homeostasis.[38] Recent studies demonstrate mechanical perturbations of the lipid bilayer alone are sufficient to activate PIEZO1 channels, demonstrating their innate properties as molecular force transducers.[39] Piezo1-deficient murine erythrocytes exhibit overhydration, suggesting a role as a negative regulator of erythrocyte volume.[40] They also demonstrate a near total lack of MA calcium influx, indicating that PIEZO1 is probably the major mechanotransducer in red blood cells. PIEZO1 activation could be mediated by transient cell swelling, a phenomenon not detected by our in vitro model. It will be exciting to tease out the contribution of PIEZO1 to volume regulation of erythrocytes as they travel through the circulation.

As shown by genome-wide association studies (GWASs), a substantial component of variability in erythrocyte hydration is genetically determined.[41,42] In normal human subjects, variation in the indices of erythrocyte hydration and volume homeostasis, including hemoglobin, cell volume, and MCHC, are strongly influenced by genetic factors.[43,44] Because numerous pathways regulate erythrocyte hydration, one would predict that any of the proteins participating in this process, from transporters and channels to their regulatory kinases and phosphatases and other important regulatory proteins, may serve as modifiers of erythrocyte

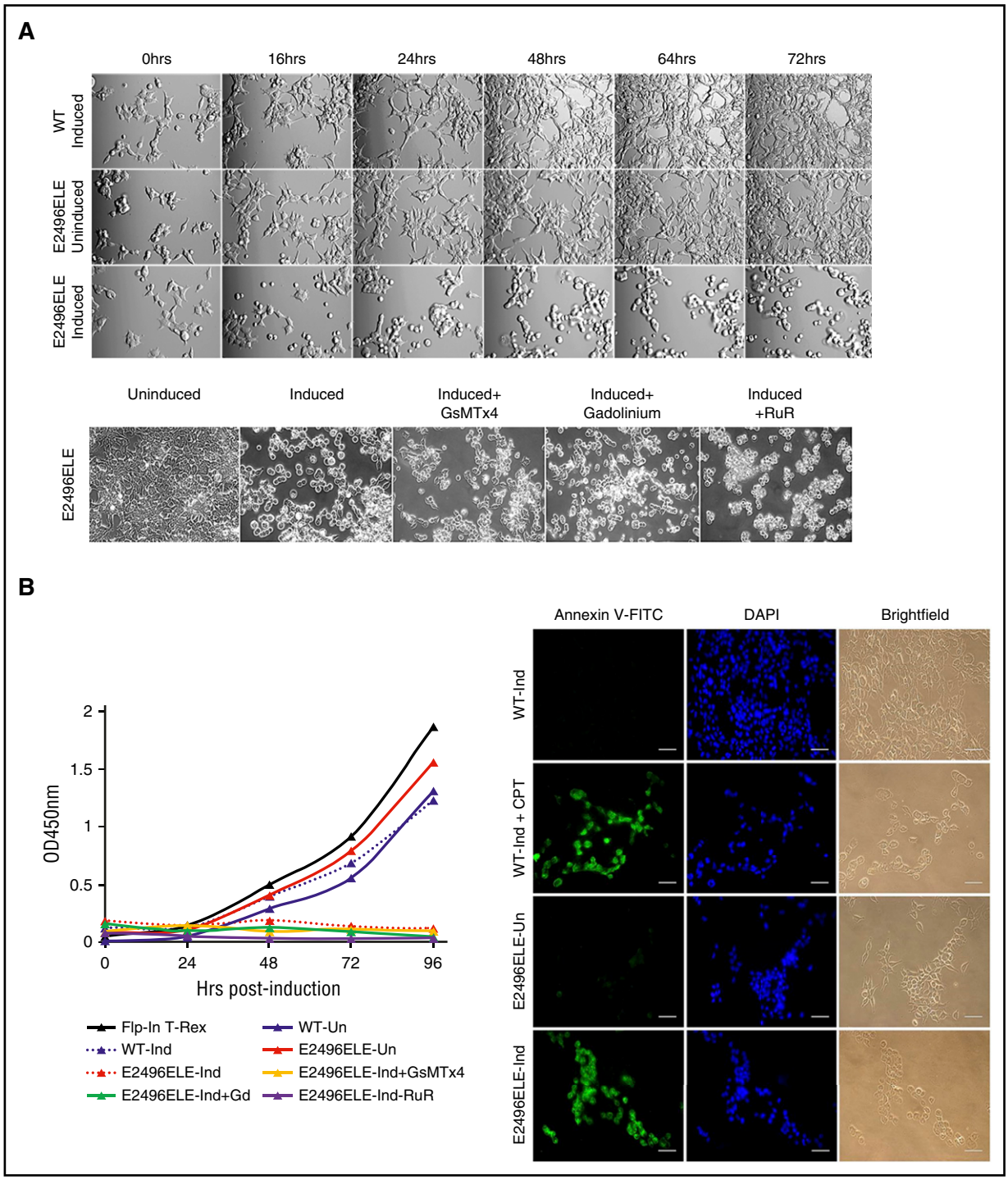

Figure 7. Studies of the E2496ELE PIEZO1 mutant. (A) HEK293 cells expressing the E2496ELE mutant displayed morphological changes upon induction. Top panels: compared with wild type, the mutant cells demonstrated swelling as early as 16 hours postinduction with rounding up of edges, followed by wide-scale detachment of cells from the plate by 48 hours. Bottom panels: none of the known PIEZO1 inhibitors, including the *G spatulata* mechanotoxin (GsMTx4), gadolinium, or ruthenium red, protected cells from this effect. Original magnification ×100. (B) Live cell numbers and annexin V staining. Beginning at ~48 hours postinduction, the number of live, mutant cell numbers determined by CCK8 staining decreased dramatically (left graph) and cells began to undergo apoptosis as assayed by annexin V staining (right). Camptothecin (CPT) was used for artificial induction of apoptosis in wild-type cells. Scale bars, 1 μm. FITC, fluorescein isothiocyanate.

hydration.[45] A GWAS of red cell indices and related parameters was performed in 135 367 individuals.[46] For MCHC, the most significant association for MCHC was a single-nucleotide polymorphism (SNP) at 16q24, rs10445033 ($P < 10e-8$). Using expression and bioinformatic strategies, this SNP, located in intron 1 of the *PIEZO1* gene locus, was linked to PIEZO1, explaining 8% of the phenotypic variance of the MCHC trait. A recent GWAS study in Hispanics and Latinos identified a different SNP in *PIEZO1* linked to MCHC.[47]

These studies indicate that variant *PIEZO1* alleles are common, some are enriched in various ethnic groups, and some are trait and/or disease-associated. Coinheritance of modifier alleles should be considered whenever a patient with a primary or secondary

erythrocyte disorder presents with an unexpectedly severe or mild clinical phenotype. Paralleling the genetic heterogeneity, mechanisms of PIEZO1 dysfunction are variable, with some yet undiscovered. Interesting observations have been made about PIEZO1 in erythrocytes, such as its role in influencing calcium and adenosine triphosphate content.[40,48] The ultimate goal is understanding the precise function(s) of wild-type and mutant PIEZO1 in erythrocytes as they travel through the high-sheer-stress circulatory system and squeeze through the hypoxic capillary bed, to then understand the precise mechanism of dehydration in HX erythrocytes.

Acknowledgments

The authors thank Mark Lessard of the Yale Cooperative Center of Excellence in Hematology (YCCEH) for technical assistance.

This work was supported in part by grants from the National Institutes of Health, National Institute of Diabetes and Digestive and Kidney Diseases (RO1DK104046 and U54DK106857), the American Society of Hematology, and the Doris Duke Research Foundation.

Authorship

Contribution: E.G. designed and performed experiments and analyzed data, with contributions from E.R.S.; K.L.-G. and Y.M. designed and performed experiments; V.P.S. analyzed data; J.W., K.R., S.B.K., D.M., A.M.F., R.A.A., and T.A.K. phenotyped, diagnosed, and collected additional information on patients; E.O.G. and S.N.B. designed experiments and analyzed data; and P.G.G. designed experiments, analyzed data, and wrote the manuscript.

Conflict-of-interest disclosure: The authors declare no competing financial interests.

Correspondence: Patrick G. Gallagher, Yale University School of Medicine, 333 Cedar St, PO Box 208064, New Haven, CT 06520-8064; e-mail: patrick.gallagher@yale.edu.

References

1. Gallagher PG. Disorders of red cell volume regulation. *Curr Opin Hematol*. 2013;20(3):201-207.
2. Archer NM, Shmukler BE, Andolfo I, et al. Hereditary xerocytosis revisited. *Am J Hematol*. 2014;89(12):1142-1146.
3. Gallagher PG, Glader BE. Hereditary spherocytosis, hereditary elliptocytosis, and other disorders associated with abnormalities of the erythrocyte membrane. In: Greer JP, Arber DA, Glader BE, et al, eds. Wintrobe's Clinical Hematology. Philadelphia, PA: Lippincot, Williams & Wilkins; 2014:707-727.
4. Glogowska E, Gallagher PG. Disorders of erythrocyte volume homeostasis. *Int J Lab Hematol*. 2015;37(suppl 1):85-91.
5. Houston BL, Zelinski T, Israels SJ, et al. Refinement of the hereditary xerocytosis locus on chromosome 16q in a large Canadian kindred. *Blood Cells Mol Dis*. 2011;47(4):226-231.
6. Andolfo I, Alper SL, De Franceschi L, et al. Multiple clinical forms of dehydrated hereditary stomatocytosis arise from mutations in PIEZO1. *Blood*. 2013;121(19):3925-3935.
7. Shmukler BE, Vandorpe DH, Rivera A, Auerbach M, Brugnara C, Alper SL. Dehydrated stomatocytic anemia due to the heterozygous mutation R2456H in the mechanosensitive cation channel PIEZO1: a case report. *Blood Cells Mol Dis*. 2014;52(1):53-54.
8. Albuisson J, Murthy SE, Bandell M, et al. Dehydrated hereditary stomatocytosis linked to gain-of-function mutations in mechanically activated PIEZO1 ion channels. *Nat Commun*. 2013;4:1884.
9. Zarychanski R, Schulz VP, Houston BL, et al. Mutations in the mechanotransduction protein PIEZO1 are associated with hereditary xerocytosis. *Blood*. 2012;120(9):1908-1915.
10. Beneteau C, Thierry G, Blesson S, et al. Recurrent mutation in the PIEZO1 gene in two families of hereditary xerocytosis with fetal hydrops. *Clin Genet*. 2014;85(3):293-295.
11. Bae C, Gnanasambandam R, Nicolai C, Sachs F, Gottlieb PA. Xerocytosis is caused by mutations that alter the kinetics of the mechanosensitive channel PIEZO1. *Proc Natl Acad Sci USA*. 2013;110(12):E1162-E1168.
12. Glogowska E, Lezon-Geyda K, Maksimova Y, Schulz VP, Gallagher PG. Mutations in the Gardos channel (KCNN4) are associated with hereditary xerocytosis. *Blood*. 2015;126(11):1281-1284.
13. Bakeer N, Luo HY, Grimley M, et al. Hemoglobin Cincinnati: a novel beta globin gene mutation causing dominant beta thalassemia. *Pediatr Blood Cancer*. 2014;61:S15.
14. Coste B, Mathur J, Schmidt M, et al. Piezo1 and Piezo2 are essential components of distinct mechanically activated cation channels. *Science*. 2010;330(6000):55-60.
15. Coste B, Xiao B, Santos JS, et al. Piezo proteins are pore-forming subunits of mechanically activated channels. *Nature*. 2012;483(7388):176-181.
16. Bae C, Gottlieb PA, Sachs F. Human PIEZO1: removing inactivation. *Biophys J*. 2013;105(4):880-886.
17. Rinehart J, Maksimova YD, Tanis JE, et al. Sites of regulated phosphorylation that control K-Cl cotransporter activity. *Cell*. 2009;138(3):525-536.
18. Kircher M, Witten DM, Jain P, O'Roak BJ, Cooper GM, Shendure J. A general framework for estimating the relative pathogenicity of human genetic variants. *Nat Genet*. 2014;46(3):310-315.
19. Imashuku S, Muramatsu H, Sugihara T, et al. PIEZO1 gene mutation in a Japanese family with hereditary high phosphatidylcholine hemolytic anemia and hemochromatosis-induced diabetes mellitus. *Int J Hematol*. 2016;104(1):125-129.
20. Coste B, Murthy SE, Mathur J, et al. Piezo1 ion channel pore properties are dictated by C-terminal region. *Nat Commun*. 2015;6:7223.
21. Ge J, Li W, Zhao Q, et al. Architecture of the mammalian mechanosensitive Piezo1 channel. *Nature*. 2015;527(7576):64-69.
22. Zhao Q, Wu K, Geng J, et al. Ion permeation and mechanotransduction mechanisms of mechanosensitive Piezo channels. *Neuron*. 2016;89(6):1248-1263.
23. Bagriantsev SN, Gracheva EO, Gallagher PG. Piezo proteins: regulators of mechanosensation and other cellular processes. *J Biol Chem*. 2014;289(46):31673-31681.
24. Michelsen K, Yuan H, Schwappach B. Hide and run. Arginine-based endoplasmic-reticulum-sorting motifs in the assembly of heteromultimeric membrane proteins. *EMBO Rep*. 2005;6(8):717-722.
25. Quilty JA, Li J, Reithmeier RA. Impaired trafficking of distal renal tubular acidosis mutants of the human kidney anion exchanger kAE1. *Am J Physiol Renal Physiol*. 2002;282(5):F810-F820.
26. Quilty JA, Reithmeier RA. Trafficking and folding defects in hereditary spherocytosis mutants of the human red cell anion exchanger. *Traffic*. 2000;1(12):987-998.
27. Zerangue N, Malan MJ, Fried SR, et al. Analysis of endoplasmic reticulum trafficking signals by combinatorial screening in mammalian cells. *Proc Natl Acad Sci USA*. 2001;98(5):2431-2436.
28. Ma D, Jan LY. ER transport signals and trafficking of potassium channels and receptors. *Curr Opin Neurobiol*. 2002;12(3):287-292.
29. Gudipaty SA, Lindblom J, Loftus PD, et al. Mechanical stretch triggers rapid epithelial cell division through Piezo1. *Nature*. 2017;543(7643):118-121.
30. Stamatoyannopoulos G, Woodson R, Papayannopoulou T, Heywood D, Kurachi S. Inclusion-body beta-thalassemia trait. A form of beta thalassemia producing clinical manifestations in simple heterozygotes. *N Engl J Med*. 1974;290(17):939-943.
31. Yang E, Voelkel EB, Lezon-Geyda K, Schulz VP, Gallagher PG. Hemoglobin C trait accentuates erythrocyte dehydration in hereditary xerocytosis. *Pediatr Blood Cancer*. 2017;64(8).
32. Andolfo I, Russo R, Manna F, et al. Novel Gardos channel mutations linked to dehydrated hereditary stomatocytosis (xerocytosis). *Am J Hematol*. 2015;90(10):921-926.
33. Roux BT, Cottrell GS. G protein-coupled receptors: what a difference a 'partner' makes. *Int J Mol Sci*. 2014;15(1):1112-1142.
34. Hebert DN, Molinari M. In and out of the ER: protein folding, quality control, degradation, and related human diseases. *Physiol Rev*. 2007;87(4):1377-1408.
35. Mohandas N. To shrink or not to shrink. *Blood*. 2013;121(19):3783-3784.
36. Delmas P, Hao J, Rodat-Despoix L. Molecular mechanisms of mechanotransduction in mammalian sensory neurons. *Nat Rev Neurosci*. 2011;12(3):139-153.
37. Pedersen SF, Kapus A, Hoffmann EK. Osmosensory mechanisms in cellular and systemic volume regulation. *J Am Soc Nephrol*. 2011;22(9):1587-1597.

38. Hua SZ, Gottlieb PA, Heo J, Sachs F. A mechanosensitive ion channel regulating cell volume. *Am J Physiol Cell Physiol*. 2010;298(6):C1424-C1430.

39. Syeda R, Florendo MN, Cox CD, et al. Piezo1 channels are inherently mechanosensitive. *Cell Reports*. 2016;17(7):1739-1746.

40. Cahalan SM, Lukacs V, Ranade SS, Chien S, Bandell M, Patapoutian A. Piezo1 links mechanical forces to red blood cell volume. *eLife*. 2015;4:e07370.

41. Ganesh SK, Zakai NA, van Rooij FJ, et al. Multiple loci influence erythrocyte phenotypes in the CHARGE Consortium. *Nat Genet*. 2009;41(11):1191-1198.

42. Kamatani Y, Matsuda K, Okada Y, et al. Genome-wide association study of hematological and biochemical traits in a Japanese population. *Nat Genet*. 2010;42(3):210-215.

43. Soranzo N, Spector TD, Mangino M, et al. A genome-wide meta-analysis identifies 22 loci associated with eight hematological parameters in the HaemGen consortium. *Nat Genet*. 2009;41(11):1182-1190.

44. Ferreira MA, Hottenga JJ, Warrington NM, et al. Sequence variants in three loci influence monocyte counts and erythrocyte volume. *Am J Hum Genet*. 2009;85(5):745-749.

45. Gallagher PG. Transporting down the road to dehydration. *Blood*. 2015;126(26):2775-2776.

46. van der Harst P, Zhang W, Mateo Leach I, et al. Seventy-five genetic loci influencing the human red blood cell. *Nature*. 2012;492(7429):369-375.

47. Hodonsky CJ, Jain D, Schick UM, et al. Genome-wide association study of red blood cell traits in Hispanics/Latinos: The Hispanic Community Health Study/Study of Latinos. *PLoS Genet*. 2017;13(4):e1006760.

48. Cinar E, Zhou S, DeCourcey J, Wang Y, Waugh RE, Wan J. Piezo1 regulates mechanotransductive release of ATP from human RBCs. *Proc Natl Acad Sci USA*. 2015;112(38):11783-11788.

2017 130: 1845-1856
doi:10.1182/blood-2017-05-786004 originally published online July 17, 2017

Novel mechanisms of PIEZO1 dysfunction in hereditary xerocytosis

Edyta Glogowska, Eve R. Schneider, Yelena Maksimova, Vincent P. Schulz, Kimberly Lezon-Geyda, John Wu, Kottayam Radhakrishnan, Siobán B. Keel, Donald Mahoney, Alison M. Freidmann, Rachel A. Altura, Elena O. Gracheva, Sviatoslav N. Bagriantsev, Theodosia A. Kalfa and Patrick G. Gallagher

Blood (print ISSN 0006-4971, online ISSN 1528-0020), is published weekly by the American Society of Hematology, 2021 L St, NW, Suite 900, Washington DC 20036.

Supplemental Data

Genetic Studies. Whole exome sequencing was performed on peripheral blood-derived genomic DNA. Whole-exome sequencing data were aligned to the human genome (hg19) and analyzed. Mean target coverage was high, 67, and >95% of all targeted bases were read more than 10X. Genotypes for single nucleotide and indel variants were called using the GATK Haplotype Caller and submitted to the Annovar annotation pipeline.

Physiologic studies. Mechanically activated currents were measured in induced and uninduced HEK293 cells expressing wild type or mutant PIEZO1 and mock transfected cells. Force was applied to the cell surface by a glass probe mounted on a piezoelectric driven actuator (Physik Instrumente) in a series of 150 ms mechanical steps, in 1 μm increments, while monitoring transmembrane currents at -80 mV in the whole cell mode as described.[14,15] Similar to previous reports, this was accomplished using a pipette driven by a Clampex controlled piezo-electric crystal microstage (Physik). Mechanically activated inward currents, apparent threshold of mechanical activation, and time constant of inactivation, obtained by fitting the inactivating component of the mechano-current to the mono-exponential equation, were monitored.

The inactivation kinetics of MA currents recorded from HEK293 cells expressing wild type and mutant PIEZO1 were best fitted with a mono-exponential function. The time constant for inactivation (τ) was calculated using the exponential standard of Chebyshev fitting method, as indicated in equation:

$$f(t) = \sum_{i=1}^{n} A_i e^{-t/\tau_i} + C$$

where A is the amplitude of measured current, τ is the time constant of inactivation, and C is the constant y-offset (instrumental offset) for each channel type i.

Immunofluorescence (IF). For the first set of IF experiments examining possible endoplasmic reticulum localization of PIEZO1 mutants: *PIEZO1 staining*: IAB: mouse anti-Flag Tag, M2 (Sigma), 1:100, 2hrs, RT; IIAB: goat anti-mouse IgG (H+L), AF555 (Thermo Fisher), 1:500, 1.5hr, RT. *ER staining*: ER-GFP conjugate with Alexa Fluor488 (Thermo Fisher), 1:500, o/n, 4^0C. For the second set of IF experiments examining possible Golgi localization of PIEZO1 mutants: *PIEZO1 staining:* IAB: mouse anti-Flag Tag, M2 (Sigma), 1:100, 2hrs, RT; IIAB: goat anti-mouse IgG, ATTO647N (Sigma), 1:1000, 1.5hr, RT; *ER staining:* Anti-Calnexin [AF18] Alexa Fluor488 (Abcam), 1:500, o/n, 4^0C; *Nucleus staining:* DAPI 1:1000, 15min, RT

Quantitative Fluorescent Western Blotting. Antibody concentrations and signal intensities were balanced and optimized prior testing samples to avoid crosstalk between channels. 40μg of erythrocyte ghosts were diluted in 2X running Buffer (2% SDS, 5% Sarkosyl, 26.3% Glycerol, 65.8 mM Tris-HCl, pH-6.6, 0.715M B-ME) and denatured at 95°C for 6 min. Denatured samples were loaded and ran on precast TGX stain-free, Any kD gels (BioRad) 200V for 30 min. Then gels were transferred to Immun-Blot LF PVDF Membrane (BioRad, cat. # 1620260) using Trans-Blot Turbo Transfer System (BioRad) (2.5A, 25V, 10 min) and blocked in 5% BSA/ 1X TBST for 30 min at room temperature. Incubation with primary antibody was carried at 4°C overnight, secondary – RT for 3 hours. Gels were imaged and quantified using ChemiDoc MP Imaging System (BioRad) and Image Lab Software.

Antibody Used for Quantitative Fluorescent Western Blotting. Primary- YU-289, anti-Piezo1 rabbit polyclonal antibody (Gallagher Lab) (1:100); 2°- anti-rabbit DyLight649 (VectorLabs, DL-1649) (1:500). Primary- C-15, anti-ACTB mouse monoclonal antibody (sc-69879) (1:5000); Secondary- anti-mouse DyLight549 (VectorLabs, DL-2549) (1:1000). Primary- RG/26, anti-Spectrin mouse monoclonal antibody (sc-53444) (1:500); 2°- anti-mouse DyLight549 (VectorLabs, DL-2549) (1:500).

Supplemental Figures

Supplemental Figure S1. PIEZO1 expression. HEK293 cells expressing wild type or mutant PIEZO1 with or without a COOH-terminal 3X FLAG tag were induced with doxycycline for 48 hours. Western blot analysis of cell lysates revealed all mutants expressed PIEZO1 protein at levels similar to wild type levels of expression.

Supplemental Figure S2. PIEZO1 localization. Immunofluorescence studies localized wild type and mutant PIEZO1 expression to the cell membrane after doxycycline induction. DAPI stain of nuclei (blue), phalloidin AF488 stain of F-actin (green), and ATT0647N Flag-tagged PIEZO1 (red) images in induced cells are shown. Scale bars: 10μM.

Supplemental Figure S3. Mechanically activated currents in HEK293 cells expressing wild type PIEZO1 without or with a COOH-terminal 3X FLAG tag.
Left. Representative traces of mechanically activated inward currents from uninduced or induced stably-transfected HEK293 cells expressing wild type PIEZO1. Using a patch-clamp electrophysiological technique, functionality of recombinant PIEZO1 channel activity was examined in the whole-cell configuration. Upon series of mechanical stimulation of a glass probe (1 μm increments, 150 ms step duration), currents were recorded in the whole-cell patch clamp configuration at holding potential -80 mV. **Middle**: Recordings from HEK293 cells expressing PIEZO1 without a FLAG tag. **Right**. Recordings from HEK293 cells expressing PIEZO1 with a COOH-terminal FLAG tag. All stimulus waveforms, shown above the current tracings, are shown on the left, whereas those that did not generate channel response were removed from the ramp in the middle and right tracing.

Supplemental Figure S4. Semi-quantitative Western blotting of erythrocyte ghosts from erythrocyte membranes of HX patients. (A). Erythrocyte membrane ghosts were stained with anti-PIEZO1, anti-actin, or anti-alpha spectrin. (B). Quantitation of Western blots using actin or alpha-spectrin as a reference. No differences in PIEZO1 expression were observed between wild type or mutant patients normalized against actin expression, alpha-spectrin expression, or both.

Supplemental Figure S5. Time lapse video of wild type PIEZO1 and the PIEZO1 E2496ELE mutant after induction. HEK293 cells expressing either wild type PIEZO1 or the E2496ELE PIEZO1 mutant, were plated, then induced with doxycycline. Time lapse video of changes in cell morphology and attachment was recorded for 72 hours. The mutant displayed

morphological changes as early as 16 hours post induction, followed by swelling and detachment from the plate”

Supplemental Figure S6. Attempt to rescue the PIEZO1 E2496ELE mutant phenotype. In an attempt to rescue the PIEZO1 E2496ELE mutant phenotype, wild type, full length PIEZO1, with eGFP as a marker of transfection, was transfected into mutant cells 12 hours prior to induction. Despite expression of the wild type protein (not shown), it did not *fully* rescue the abnormal morphology or the decreased live cell number phenotypes.

Supplemental Figure S1

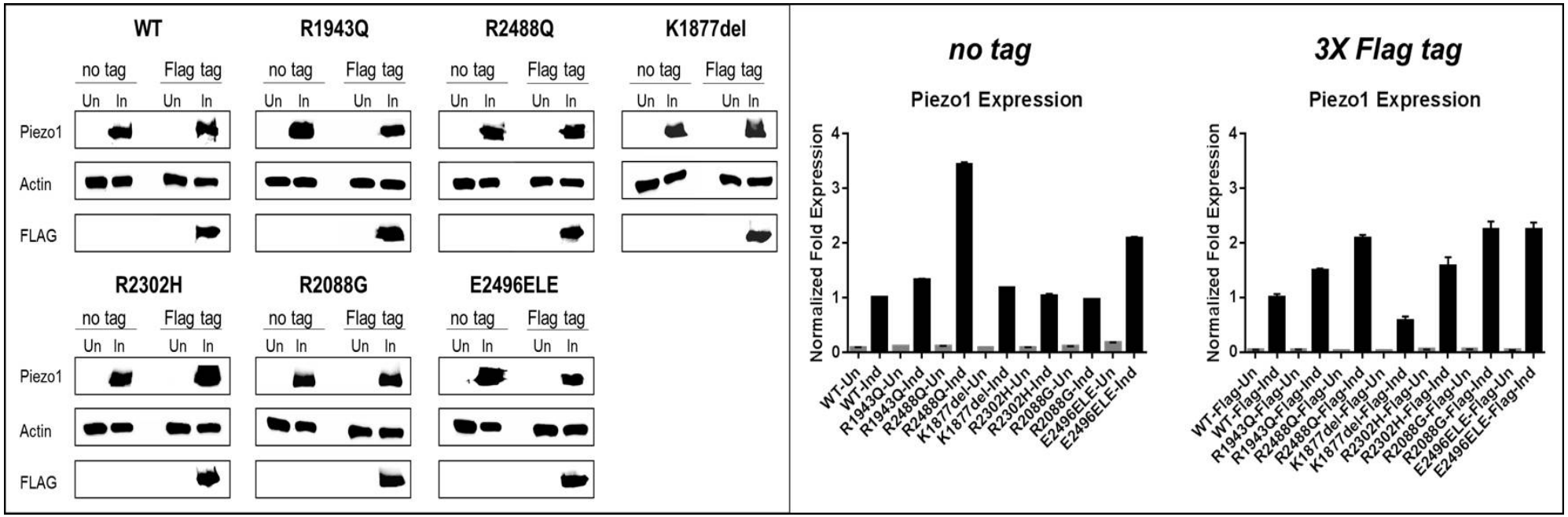

Supplemental Figure S1. PIEZO1 expression. HEK293 cells expressing wild type or mutant PIEZO1 with or without a COOH-terminal 3X FLAG tag were induced with doxycycline for 48 hours. Western blot analysis of cell lysates revealed all mutants expressed PIEZO1 protein at levels similar to wild type levels of expression.

Supplemental Figure S2

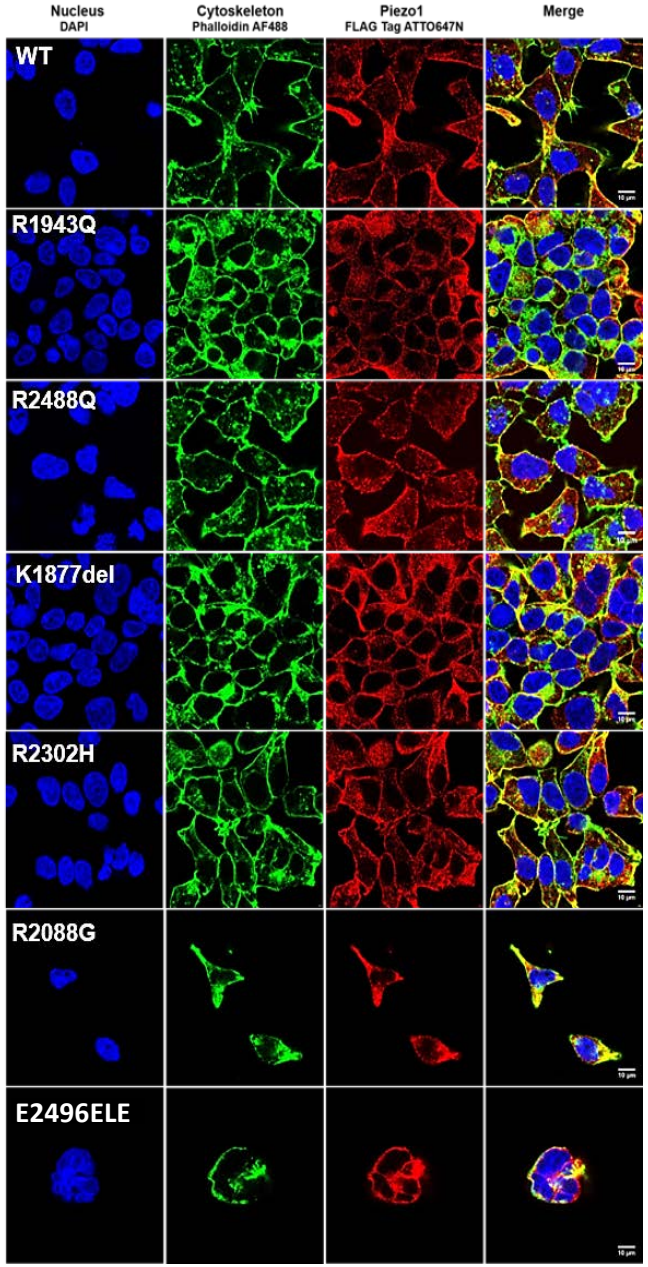

Supplemental Figure S2. PIEZO1 localization. Immunofluorescence studies localized wild type and mutant PIEZO1 expression to the cell membrane after doxycycline induction. DAPI stain of nuclei (blue), phalloidin AF488 stain of F-actin (green), and ATT0647N Flag-tagged PIEZO1 (red) images in induced cells are shown. Scale bars: 10µM.

Supplemental Figure S3

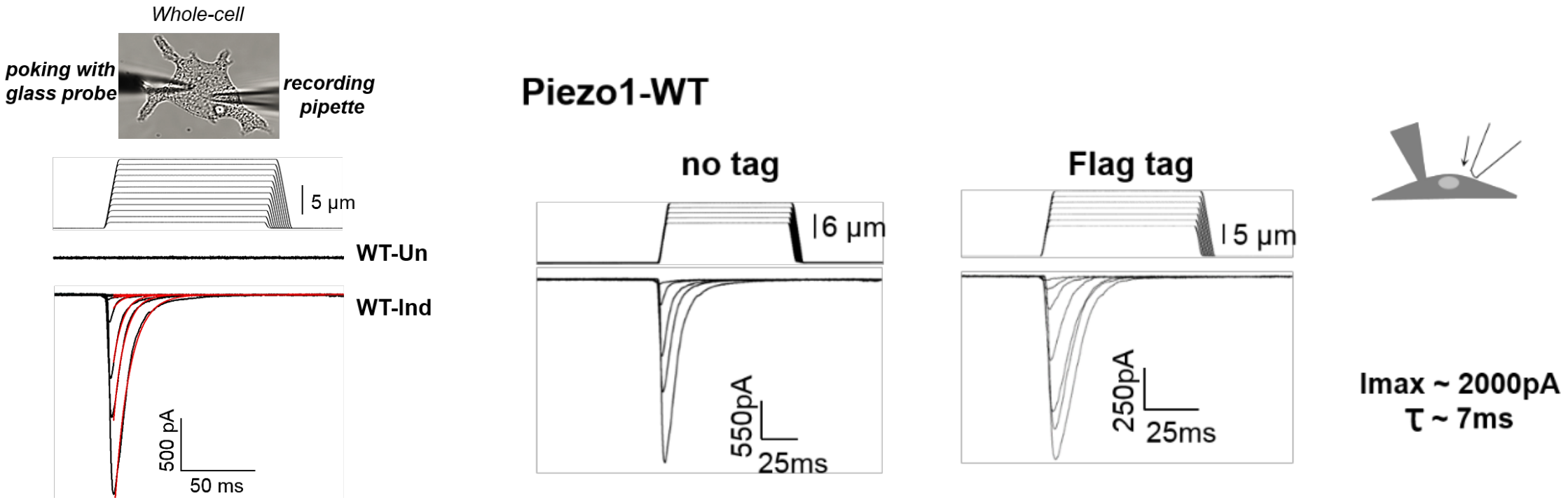

Supplemental Figure S3. Mechanically activated currents in HEK293 cells expressing wild type PIEZO1 without or with a COOH-terminal 3X FLAG tag. **Left.** Representative traces of mechanically activated inward currents from uninduced or induced stably-transfected HEK293 cells expressing wild type PIEZO1. Using a patch-clamp electrophysiological technique, functionality of recombinant PIEZO1 channel activity was examined in the whole-cell configuration. Upon series of mechanical stimulation of a glass probe (1 µm increments, 150 ms step duration), currents were recorded in the whole-cell patch clamp configuration at holding potential -80 mV. **Middle**: Recordings from HEK293 cells expressing PIEZO1 without a FLAG tag. **Right**. Recordings from HEK293 cells expressing PIEZO1 with a COOH-terminal FLAG tag. All stimulus waveforms, shown above the current tracings, are shown on the left, whereas those that did not generate channel response were removed from the ramp in the middle and right tracing.

Supplemental Figure S4A

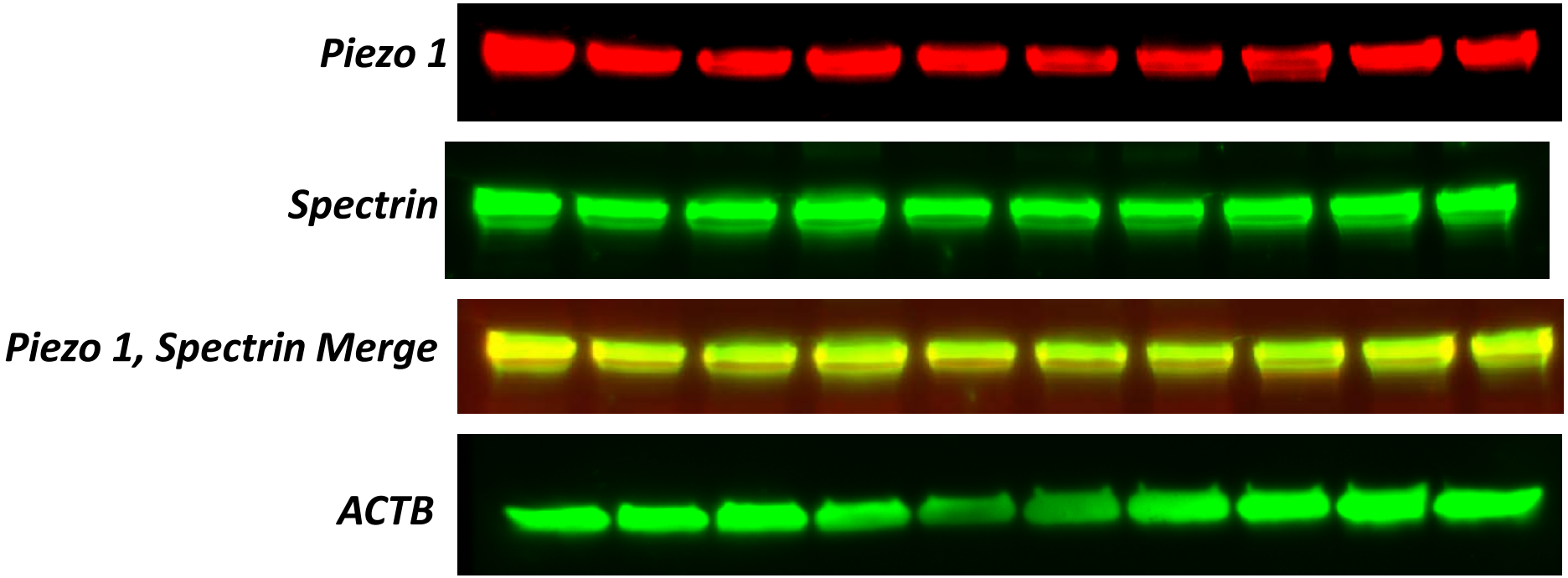

Supplemental Figure S4. Semi-quantitative Western blotting of erythrocyte ghosts from erythrocyte membranes of HX patients. (A). Ghosts were stained with anti-PIEZO1, anti-actin, or anti-alpha spectrin. (B). No differences in PIEZO1 expression were observed between wild type or mutant patients normalized against actin expression, alpha-spectrin expression, or both.

Supplemental Figure S4B

Supplemental Figure S4. Semi-quantitative Western blotting of erythrocyte ghosts from erythrocyte membranes of HX patients. (A). Membrane ghosts were stained with anti-PIEZO1, anti-actin, or anti-alpha spectrin. (B). No significant differences in PIEZO1 expression were observed between wild type or mutant patients normalized against actin expression, alpha-spectrin expression, or both.

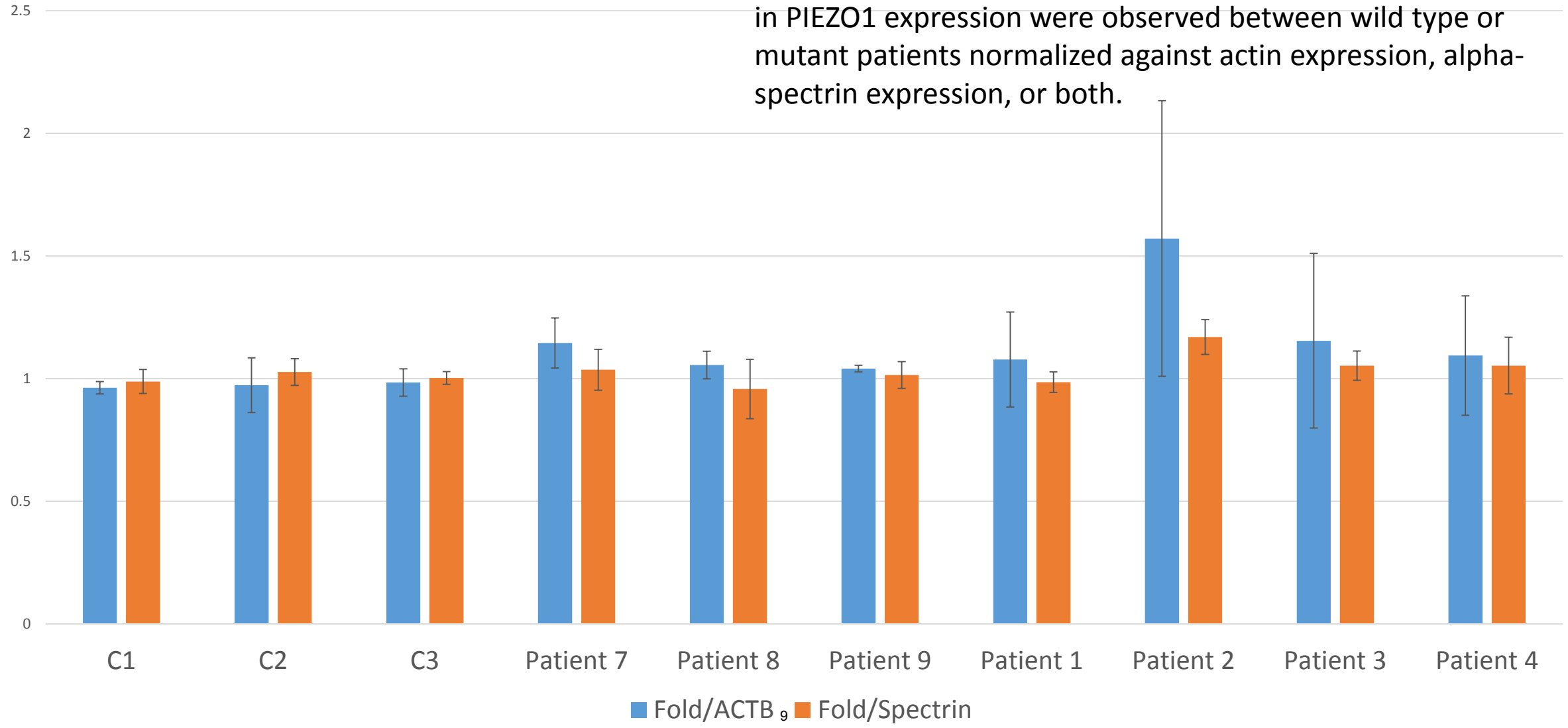

Supplemental Figure S5

Supplemental Figure S5. Time lapse video of wild type PIEZO1 and the PIEZO1 E2496ELE mutant after induction. HEK293 cells expressing either wild type PIEZO1 or the E2496ELE PIEZO1 mutant, were plated, then induced with doxycycline. Time lapse video of changes in cell morphology and attachment was recorded for

Supplemental Figure S5

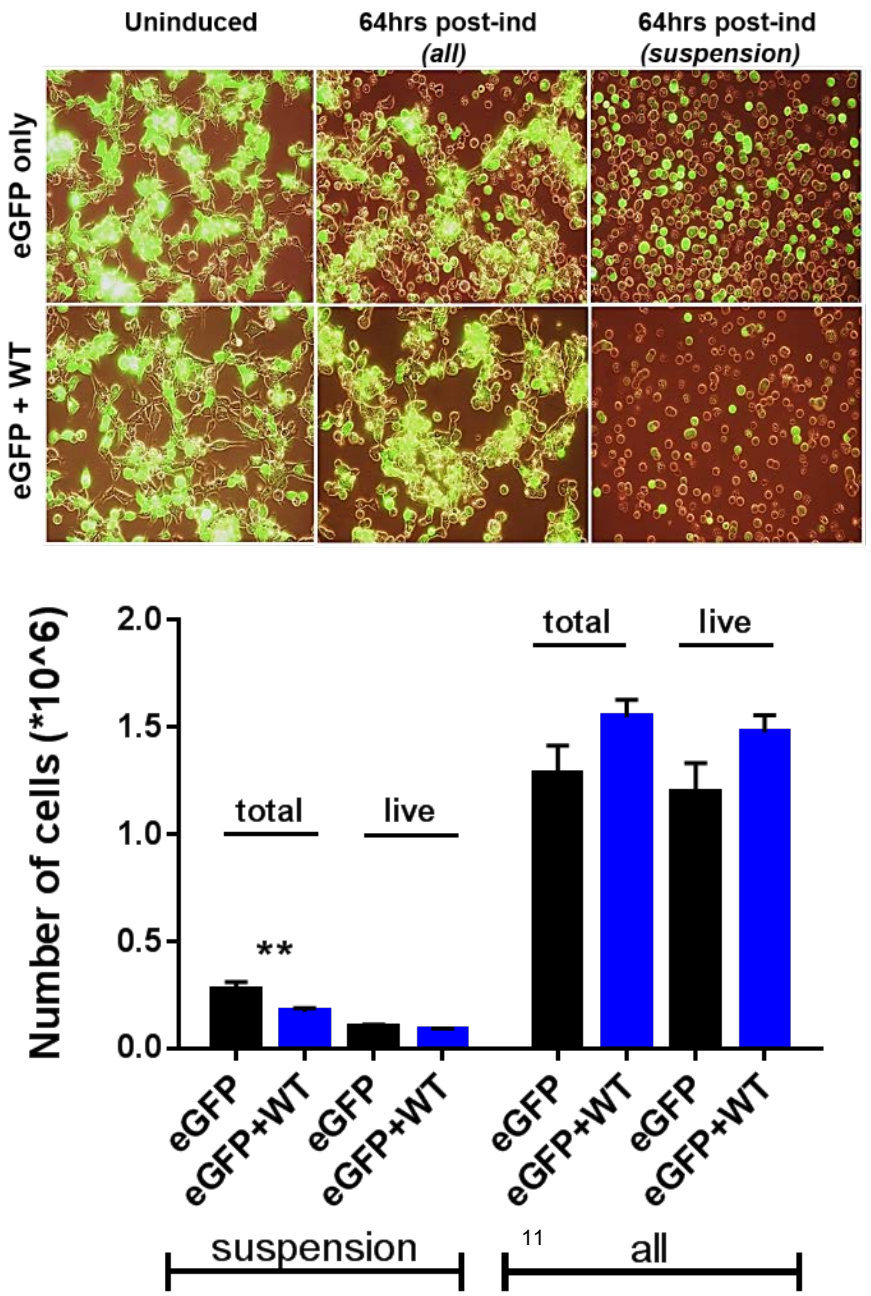

Supplemental Figure S6. Attempt to rescue the PIEZO1 E2496ELE mutant phenotype. In an attempt to rescue the PIEZO1 E2496ELE mutant phenotype, wild type, full length PIEZO1, with eGFP as a marker of transfection, was transfected into mutant cells 12 hours prior to induction. Despite expression of the wild type protein (not shown), it did not *fully* rescue the abnormal morphology or the decreased live cell number phenotypes.